Effect of membrane filtration and direct steam injection on mildly refined rapeseed protein solubility, air-water interfacial and foaming properties

Panayiotis Voudouris [a,b], Helene C.M. Mocking-Bode [a,b], Leonard M.C. Sagis [c], Constantinos V. Nikiforidis [d], Marcel B.J. Meinders [a,b], Jack Yang [a,c,d,*]

[a] *TiFN, Nieuwe Kanaal 9A, 6709 PA, Wageningen, the Netherlands*
[b] *Agrotechnology and Food Sciences Group, Wageningen Food & Biobased Research, Wageningen University & Research, Bornse Weilanden 9, 6700AA, Wageningen, the Netherlands*
[c] *Laboratory of Physics and Physical Chemistry of Foods, Wageningen University, Bornse Weilanden 9, 6708WG, Wageningen, the Netherlands*
[d] *Laboratory of Biobased Chemistry and Technology, Wageningen University, Bornse Weilanden 9, 6708WG, Wageningen, the Netherlands*

A B S T R A C T

Rapeseed is an upcoming source of alternative proteins and extensive processing is necessary to utilise these proteins as functional ingredients. A risk here is the potential alteration of proteins upon processing, such as aggregation, thus affecting final ingredient's functional properties. Therefore, we aim to evaluate processing methods that are considered 'mild' for the proteins to retain native proteins with good techno-functionality. We evaluate the impact of two upcoming processes: 1) membrane filtration (5 kDa) to remove small solutes and 2) short but high-temperature heating using direct steam injection (DSI, 4 s at 115 °C) to ensure microbial safety. These extracts were studied for their protein composition, size and hydrophobicity. We, for instance, show the presence of cruciferin and napin in the extracts, which are the two main rapeseed protein families. Membrane filtration was suitable to remove phenols and non-protein solutes (e.g. carbohydrates and minerals), thereby increasing the protein content of the protein powders from 45.1 to 63.4% (w/w). DSI led to about three times lower protein solubility (from ~44% to ~16%) due to aggregation. These aggregates were mainly formed by cruciferin proteins, while napins remained soluble. As a result, the soluble napin proteins dominated the air-water interface and foam stabilisation. At the same time, cruciferin proteins were more dominant in the non-heated extracts, as they were in a soluble non-aggregated state. We showed an improved foamability of about 10% after heating but a 30–40% decrease in foam stability. A final finding was the impact of non-protein solutes, which vastly decreased the interfacial stiffness, leading to substantially less stable foams compared to membrane-filtered samples. In this work, we demonstrate how crucial processing steps, such as heating and filtration, impact (protein) composition, molecular and functional properties, which are crucial insights in designing protein extraction processes to obtain functional protein ingredients.

1. Introduction

Rapeseed (*Brassica napus*) is a promising source of proteins for food formulations as an alternative to animal-based proteins. Such alternatives are necessary to address global sustainability and food security-related challenges (Aiking & de Boer, 2018). The seed composition is about 17–24% (w/w) protein, 40–45% (w/w) oil, and 3% (w/w) phenols (Aider & Barbana, 2011; Wanasundara, 2011). Rapeseed proteins are considered to have a balanced amino acid composition and were previously shown to have good functional properties, such as for foaming, emulsifying and gelation (Baker et al., 2022; Barbin, Natsch, & Müller, 2011; Jia, Curubeto, Rodríguez-Alonso, Keppler, & van der Goot, 2021; Ntone, Kornet, et al., 2022; Sánchez-Vioque, Bagger, Rabiller, & Guéguen, 2001; Xu et al., 2021; Yang, Berton-Carabin, Nikiforidis, van der Linden, & Sagis, 2021; Zhang et al., 2022).

Currently, rapeseeds are cultivated for canola oil, which is extracted using pressing and solvent extraction. The result of oil extraction is a side stream that is a protein-rich defatted meal (Alashi, Blanchard, Mailer, & Agboola, 2013; Nehmeh et al., 2022; Rommi et al., 2015). Proteins can be extracted from the defatted meal through the alkaline

---

extraction combined with precipitation at their iso-electric point (pI) (Chéreau et al., 2016; Sari, Mulder, Sanders, & Bruins, 2015). At alkaline pH, proteins are solubilised and extracted from the meal, while when precipitated at the pH = pI, the proteins will aggregate and precipitate. As a result, the non-proteinaceous solutes (e.g. phenols, carbohydrates and anti-nutritional factors), but non-protein nitrogen-contributing proteins (e.g. peptides and free amino acids) can be removed after centrifuging the precipitated proteins (Yang et al., 2024). The pellet is then redispersed, sometimes heated to increase microbial stability, and then freeze/spray-dried to yield a relatively pure protein extract (>80% protein purity).

Although this protein extraction method seems simple, it has major drawbacks with regard to protein functionality. Proteins in these pure protein extracts are often heavily aggregated, mostly due to three process steps: 1) the industrial defatting step requires extensive heating steps (>100 °C) to reduce enzyme activity and evaporate solvents used during oil extraction (Fetzer, Herfellner, & Eisner, 2019); 2) the iso-electric point precipitation step may induce irreversible aggregation of proteins, as shown for pea, mungbean and Bambara groundnut (Geerts, Nikiforidis, van der Goot, & van der Padt, 2017; Yang, de Wit et al., 2022; Yang, Yang, et al., 2023); and 3) the heating step before drying. Heavily aggregated proteins may lead to oil droplet coalescence, fast foam collapse and weak heterogeneous gels (Kornet, Veenemans, et al., 2021; Yang et al., 2024). Therefore, this work will explore alternative processes to omit these three aggregate-inducing steps.

The solvent defatting step can be omitted by co-extraction of both lipids and proteins in a so-called mild extraction method, previously developed for rapeseed (Ntone, Bitter, & Nikiforidis, 2020). In brief, dehulled rapeseeds were disrupted at an alkaline pH, followed by a gravitational separation step. The result is a protein-rich layer, which is also rich in other non-proteinaceous solutes, such as phenols, sugars and minerals. These non-proteinaceous solutes could negatively impact functionality in the final application or health upon consumption. An example of a negative impact is the lower foam and emulsion stabilisation by proteins in the presence of the main rapeseed phenol sinapic acid (Ntone, Qu, et al., 2022; Yang, Lamochi Roozalipour, et al., 2021). Iso-electric point precipitation is normally used to separate the non-proteinaceous components into a side stream, and it can be replaced by membrane filtration (often with a cut-off of 3–10 kDa), where the low molecular solutes can be removed, while the proteins are retained. Membrane filtration on rapeseed protein extracts was proven to be effective in the removal of anti-nutrient factors (e.g. phytates and glucosinolates) and minerals, and led to lighter protein extracts compared to one produced using iso-electric point precipitation (Fetzer et al., 2019; Tzeng, Diosady, & Rubin, 1988, 1990). A combination of mild purification and membrane filtration was previously tested on several protein sources, such as yellow pea, rapeseed and Bambara groundnut, with protein purities varying from 62.1 to 88.2% (Kornet, Shek, et al., 2021; Ntone et al., 2020; Yang, de Wit et al., 2022).

Another potential advantage of membrane filtration is the increased protein extraction yield by retention of albumin proteins. Rapeseed has two major storage protein classes, which are globulin and albumins. According to Osborne's classification (Osborne, 1924), globulins are dilute saline soluble, and albumins are water-soluble. Rapeseed proteins have a specific nomenclature, where the globulin is called cruciferin, and the albumin is called napin. Both proteins are co-extracted from the seeds, but then separated in the iso-electric point precipitations step. This step is performed at the pI of cruciferin (usually between pH 4 and 5) (Cheung, Wanasundara, & Nickerson, 2014a, Cheung, Wanasundara, & Nickerson, 2014b; Ntone et al., 2020), which causes cruciferin aggregation. While cruciferin aggregates and precipitates at the pI, napin proteins remain soluble. After a gravitational separation step, the napin proteins would remain in the supernatant, which is generally discarded. Rapeseed can contain up to 20% albumin proteins, which would be discarded using iso-electric point precipitation. Membrane filtration would, therefore, be a suitable method to co-extract napin and cruciferin into the final protein ingredient.

A final processing step is heating, which is necessary to increase microbial stability of the final ingredient, but may cause heat denaturation of proteins due to protein unfolding and subsequent aggregation (Schmitt, Silva, Amagliani, Chassenieux, & Nicolai, 2019). Heating is often performed by pasteurisation or ultra-heat treatments (UHT), which are generally indirect tubular heating methods. An upcoming method is direct steam injection (DSI), where steam of >100 °C is directly injected into the sample. These are general rapid processes with short holding times at high temperatures, such as 4 s at 115 °C in this work, also known as high-temperature short time (HTST) treatments. Previous work has shown smaller whey protein aggregate sizes when using DSI instead of tubular heating (X. Wang & Zhao, 2023b). For pea-rice protein blends, higher protein solubility was obtained after DSI, increasing from 4 to 50% at pH 9 (Pietrysiak, Smith, Smith, & Ganjyal, 2018). Therefore, we will test DSI as a heating step on the mildly extracted rapeseed protein extracts, in combination with membrane filtration.

To summarise, defatting, iso-electric point precipitation and tubular heating steps might induce protein aggregation. We aim to omit these steps by producing mildly extracted rapeseed protein extracts and introducing a combination of membrane filtration and/or heating using DSI. Membrane filtration and direct steam injection have been widely successfully applied to obtain dairy protein ingredients, and has been proven useful plant protein extraction as well, for instance, for soy bean, pea, rice and oats (Eze, Kwofie, Adewale, Lam, & Ngadi, 2022; Reig, Vecino, & Cortina, 2021; X. Wang & Zhao, 2023a), thereby showing the adaptability and transferability of these techniques. While such methods are available, the link to functionality is not evident, especially for rapeseed proteins. Therefore, the goal and novelty of this work is to these processes to alter, and ultimately enhance, protein functional properties. We will do this in a stepwise manner by first studying the protein composition and molecular propreties (e.g. solubility, size and surface hydrophobicity), and couple this to air-water interface- and foam-stabilising properties of the rapeseed proteins. Foaming properties were specifically chosen, as non-proteinaceous components and protein aggregated state immensely impact foamability and stability. This work will highlight the process-structure-function relationship, thereby providing new insights into the effects of protein extraction methods, allowing the development of new protein extraction processes, which are essential for creating sustainable and healthy food products.

2. Experimental section

2.1. Materials

Untreated Alizze rapeseeds (*Brassica napus*) were provided by a local seed producer and used as starting material. All (analytical grade) chemicals were obtained from Merck (Germany), and used as received. All samples were prepared in ultrapure water (MilliQ Purelab Ultra, Germany), unless stated otherwise.

2.2. Sample preparation

2.2.1. Preparation of rapeseed protein extracts

Mildly refined rapeseed protein extracts were produced using a method previously developed by Ntone et al. (Ntone et al., 2020) with adaptations. A schematic overview of the processes is shown in Fig. 1. Rapeseed kernels were dehulled by pin milling (DLFM, Buhler GmbH, Germany) to break the seeds in half, followed by hull removal using a fluid bed dryer (Retsch GmbH, Germany) connected to a vacuum cleaner (Turbo XL, BUFA Cleaning Systems GmbH & Co, Germany). The dehulled rapeseeds were soaked in a 1:8 (w:w) rapeseed-to-water ratio. The pH was adjusted to 9.0 using 1M NaOH and kept constant with a pH-stat (902 Titrando, Metrohm, Switzerland). Afterwards, the mixture was blended at max speed for 2 min in a Vita-Prep blender (Vitamix,
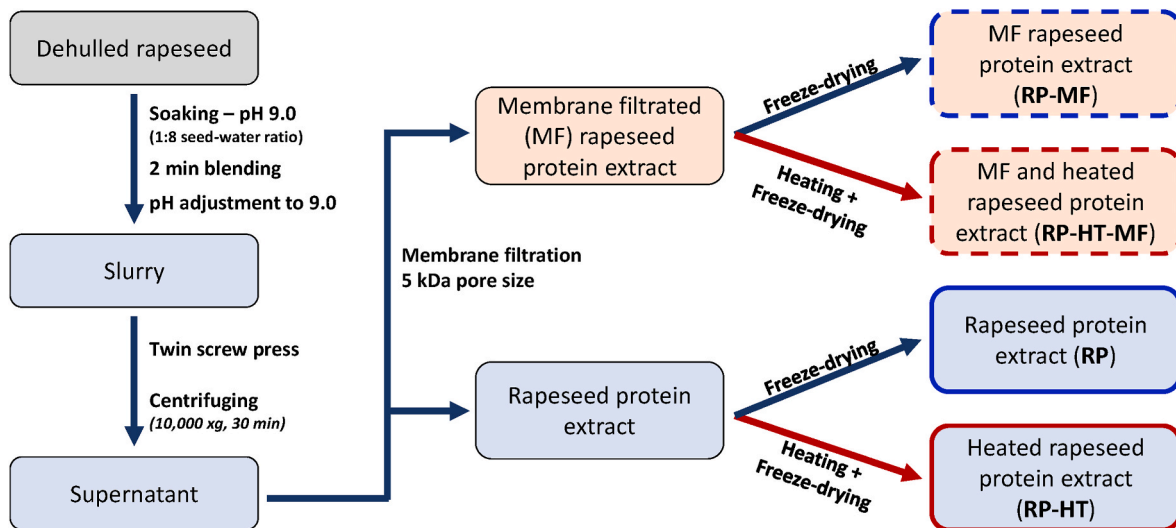
Fig. 1. Overview of protein extraction and fractionation processes applied in this work.

USA). The pH of the slurry was adjusted to pH 9 and stirred for another 1 h, while kept constant at this value with a pH-stat. The slurry was separated into a solid and liquid stream using a twin-screw press (Angelia 7500, Angle Juicer, The Netherlands). The liquid stream was centrifuged at $10,000 \times g$ for 30 min (4 °C). This step yielded a top oil-rich cream layer, a protein-rich middle layer and a fibre-rich pellet. The protein-rich middle layer was recovered and followed two routes: 1. non-membrane filtrated and 2. Membrane-filtrated. The membrane filtration was performed by pumping the liquid through two coupled diafiltration cassettes (Ntone et al., 2020) (Hydrosat, Sartorius, Germany, cut-off 5 kDa, 0.2 m^2 membrane area). A 5 kDa cut-off was chosen to retain the napin (15 kDa). Six filtration cycles (diavolume of ± 5 L) were performed with pressure-in of 3.0 bar and pressure-out of 1.8 bar, wherein in each cycle, the liquid is concentrated by half, followed by dilution with 0.08 M NaCl to avoid protein precipitation. In the last cycle, deionised water was added to remove the remaining salts. The membrane was cleaned in between using NaOH and thoroughly rinsed with demi-water before further use.

In both routes (non-membrane and membrane-filtrated), half of the material was heated in an HT220 high-temperature short time – ultra heat treatment (HTST/UHT) system (OMVE, Netherlands). First, the sample was preheated to 65 °C, followed by direct steam injection (DSI) to reach and hold for 4 s at 115 °C at a flow rate of 30L/h. The other half of the material did not receive any heat treatment. All streams were then homogenised at 20/4 (first/second stage) MPa (or 200/40 bar) for 1 pass, followed by freeze-drying. The homogenisation step was added to break down formed aggregates, mostly formed after heating. The result is a 1) non-heated and non-membrane filtrated rapeseed protein extract (RP), 2) a non-heated and membrane filtrated rapeseed protein extract (RP-MF), 3) a heated and non-membrane filtrated rapeseed protein extract (RP-HT) and 4) a heated and membrane filtrated rapeseed protein extract (RP-HT-MF).

2.2.2. Compositional analysis

The compositional analysis was performed on all protein extracts. The protein content analysis was also performed on the starting material (dehulled rapeseeds).

Protein content was calculated by determining the nitrogen content using a FLASH EA 1112 series Dumas (Interscience, the Netherlands). The nitrogen conversion factor was 5.7 (Mariotti, Tomé, & Mirand, 2008). Each sample was measured in triplicate.

The oil content was analysed using a Soxhlet extraction method (Yang, Vardar, Boom, Bitter, & Nikiforidis, 2023). Oil was extracted from 2 to 3 g of material by a 16 h extraction step using petroleum ether as a solvent. The oil content of each sample was determined in triplicate.

The phenol content was determined using a Folin-Ciocalteu assay (Ozdal, Capanoglu, & Altay, 2013). Sinapic acid was used to create a calibration curve. The phenol was dissolved in MilliQ water in a concentration range of 0.001–0.01% (w/w). The rapeseed protein extracts were similarly dissolved in MilliQ water at dry matter concentrations between 0.01 and 0.5 % (w/w). Aliquots of 1 mL of samples were diluted with 5 mL of MilliQ water, followed by adding 0.4 mL of Folin Ciocalteu reagent. After vortexing, 1 mL of a saturated Na_2CO_3 solution was added, and the total volume in the flask was increased to 10.0 mL using MilliQ water. After another vortex step, the samples were incubated at room temperature in the dark for 1 h. The samples were vortexed once more before measuring their absorbance at 725 nm. All samples were prepared in triplicate.

The moisture content was determined by heating aliquots of 30 g at 105 °C for 24 h to determine the moisture content of the powder. Afterwards, the powders were heated further slowly to 550 °C with a holding time of 6 h, and the ash content was quantified gravimetrically and expressed based on dry matter (Romero-Guzmán, Köllmann, Zhang, Boom, & Nikiforidis, 2020).

The carbohydrate content was calculated by subtracting the sum of protein, oil, phenol and ash from 100%.

2.2.3. Determination of protein solubility

The protein solubility was determined using an adapted method from (Gonzalez-Perez, Vereijken, van Koningsveld, Gruppen, & Voragen, 2005). Protein extracts were dissolved at a protein concentration of 0.1% (w/w) in MilliQ water and slowly stirred for 1 h, while the pH was constantly (every 15 min) adjusted to 7.0 using 0.1 M NaOH or HCl. Then, the samples were stored at 4 °C overnight (16 h). The following day, the samples were adjusted to pH 7.0 and centrifuged at $15,000 \times g$ for 10 min. The supernatant was filtered over a 0.45 μm syringe filter. The protein solubility was for the first time determined using Dumas and Bradford assay simultaneously to create a calibration curve for the Bradford assay. For the Bradford assay, cuvettes were filled with 3.0 mL of sample and 0.1 mL of Bradford reagent. The cuvettes were carefully rotated and incubated for 5 min at room temperature in the dark. A calibration curve with 0–0.1% bovine serum albumin (>98% solubility). After incubation, the absorbance was measured at a wavelength of 595 nm. All samples were prepared in triplicate.

2.2.4. Sample preparation of protein solutions

Protein solutions based on the protein content of the powders were produced by dissolving the amount of proteins directly in the solution.

Protein solutions based on *soluble* protein content were corrected for the soluble protein content, determined by 2.2.3. In both cases, a similar overnight dissolving method was used, as mentioned in 2.2.3, and samples were adjusted to pH 7.0. For the solution based on soluble protein, the sample was centrifugated and filtrated (same method as in 2.2.3.), as described in section 2.2.3, and the solubility was checked using Bradford. The samples were used within 24 h, and stored at 4 °C, if not directly used.

2.3. Protein composition by SDS-PAGE

The protein composition of the rapeseed protein extracts was analysed using sodium dodecyl sulfate – polyacrylamide gel electrophoresis (SDS-PAGE) under reducing conditions from InVitrogen Novex (ThermoFischer Scientific, USA). Protein solutions with 0.1% (w/w) were produced based on the full extract (insoluble proteins not removed). Also, solutions with 0.1% soluble proteins were included in the analysis. The samples were mixed with 500 mM DTT and NuPAGE LDS buffer. The samples were heated for 10 min at 70 °C and loaded on a 4–12% (w/w) BisTris gel. A marker with a molecular weight range from 2.5 to 200 kDa was included. The electrophoresis step was performed for about 30 min at 200 V. The gel was stained with SimplyBlue Safestain and analysed using a gel scanner.

2.4. Protein particle size by laser diffraction

The particle size distribution of 0.1% (w/w) rapeseed protein extract solutions (including soluble and insoluble fraction) at pH 7.0 was analysed using a Master sizer 2000/3000 (Malvern Instruments Ltd, UK). Refractive indices of 1.45 and 1.330 for the blue laser (470 nm) were used for the dispersed phase (protein) and dispersant (demineralised water), respectively. All measurements were performed in triplicate.

2.5. Protein surface hydrophobicity

The protein surface hydrophobicity was analysed using an ANSA method (Xia, Botma, Sagis, & Yang, 2022), which is a fluorescent probe 8-anilino-1-naphthalene sulfonic acid ammonium salt. Protein solutions were prepared with a soluble protein content ranging from 0.005 to 0.04% (w/w). Aliquots of 3 mL protein solution were transferred into a 4 mL cuvette. Afterwards, 25 mL of an 8 mM ANSA solution was added, followed by careful mixing by rotation and incubation at room temperature in the dark for 1 h. Then, the cuvettes were analysed using a fluorimeter LS 50B luminescence spectrometer (PerkinElmer, USA). The excitation and emission wavelength were set at 390 and 470 nm, respectively, with slit gaps at 5 mm. A 0% (w/w) protein solution was used as a blank. The slope of the emission intensity versus soluble protein concentration was a measure of the protein hydrophobicity, where a higher slope indicates higher protein solubility. Two independent samples were prepared for each protein extract, and each replicate was analysed twice.

2.6. Protein denaturation properties

The method for denaturation properties was based on (Pelgrom, Boom, & Schutyser, 2014), with adaptations. Samples were prepared by dissolving 20% (w/w) of rapeseed protein extracts (based on the dry matter) in MilliQ water for 16 h and adjusted to pH 7.0. About 30 mg of the sample was transferred to high-volume stainless steel pans. The pans were measured in a TA Q200 Differential Scanning Calorimeter (TA Instruments, New Castle, USA). The pans were equilibrated for 5 min at 20 °C, followed by a heating step from 20 to 130 °C with a heating rate of 5 °C/min. All samples were measured in triplicate.

2.7. Air-water interfacial properties

Air-water interfacial properties were determined using a drop tensiometer PAT-1M (Sinterface Technologies, Germany). The method is based on (Van Kempen, Schols, Van Der Linden, & Sagis, 2013), with adaptations. Solutions with 0.1% (w/w) soluble protein were prepared and pumped into the system to create a pendant/hanging water droplet at the tip of a straight needle. The droplet's shape was monitored by a camera and fitted with a Young-Laplace equation, giving the surface tension. The surface tension was analysed for 1 h at a constant droplet area of 20 mm^2.

After the 1 h waiting phase, the droplet was subjected to dilatational oscillatory deformations in so-called amplitude sweeps. Here, the deformation amplitude was increased from 5 to 30% at a frequency of 0.02 Hz. Five cycles of each amplitude (total 250 s) were performed, and a pause step of 50 s was present between each amplitude step increase. All measurements were performed in triplicate at 20 °C.

Non-linearities in the raw signal were further analysed by creating Lissajous plots. The surface pressure $\Pi = \gamma$-γ_0 was plotted versus the deformation $(A$-$A_0)/A_0$, where γ and A are the surface tension and area of the droplet's deformed interface, and γ_0 and A_0 are the surface tension and area of the non-deformed interface, respectively. The middle three oscillations of each amplitude were used to create the plots.

2.8. Interfacial film thickness by ellipsometry

The protein-stabilised interfacial film thickness was studied using an imaging nulling ellipsometer (EP4, Accurion, Germany). The method is based on (Peng et al., 2024). Air-water interfacial films were created in a 60 mm diameter Petri dish by injecting 10 mL of 0.1% (w/w) soluble protein solution. The air-water interfaces were equilibrated for 1 h while being covered to minimise water evaporation. The interfacial films were analysed by measuring the intensity and polarization change of an incident-polarised laser light beam with wavelengths ranging from 499.8 to 793.8 nm. This analysis was performed over two zones at an angle of incidence of 50° to obtain the ellipsometric parameters phase shift (δ) and amplitude ratio (ψ). The analysis was performed at room temperature, and the output was fitted using EP4Model v.3.6.1. software. A model was used with three layers: the substrate buffer, the ambient medium air, and the intermediate protein film layer. The parameters of the protein layer in the model were fitted using a Cauchy model (equation (1)).

$$n(\lambda) = A + \frac{B}{\lambda^2} + \frac{C}{\lambda^4} \tag{1}$$

Where n is the refractive index; λ is the wavelength of the polarised light; A, B, and C are fitting parameters. Three films were created in separate Petri dishes, which were each measured once.

2.9. Foam properties

The foaming methods were based on (Yang, Kornet, et al., 2022). Foams were created by whipping 15 mL of 0.1% (w/w) protein solution for 2 min at 2000 rpm with an aerolatte froth (Aerolatte, UK) connected to an overhead stirrer. The foams were created in a plastic tube (3.4 cm diameter). The top and bottom of the foams were directly marked on the tubes, and the foam height was measured with a ruler. The foam height and tube diameter were converted into foam volume. The foamability was expressed as the foam overrun (%), which was calculated by equation (3).

$$Foam\ overrun\ (\%) = \frac{Foam\ volume\ (mL)}{Initial\ liquid\ volume\ (15\ mL)}\ x\ 100 \tag{3}$$

After determining the initial foam volume, the foam was transferred into a 50 mL glass cylinder and covered by parafilm. The foam volume

was recorded every 5 min until half of the initial foam volume had collapsed, which is known as the foam half-life time. The experiments were performed in triplicate at room temperature.

2.10. Statistical analysis

The statistical significance between the samples was evaluated using a one-way analysis of variance (ANOVA) and Duncan's test at p ≤ 0.05, using SPSS 25.0 software (SPSS Inc., USA).

3. Results and discussion

3.1. Composition and molecular properties of the extracts

3.1.1. Composition

The rapeseed protein extracts were produced using the schematic overview of processes presented in Fig. 1(Ntone et al., 2020). Dehulled rapeseeds were soaked in alkaline water (pH 9), followed by pressing and centrifugation to obtain a protein-rich supernatant, yielding a rapeseed protein extract (RP) with a protein content of 45.1% (w/w) (Table 1). An additional 14.5% (w/w) oil, in the form of oleosomes, was present, as the rapeseeds were not defatted (Ntone et al., 2020). The RP was also heat-treated (before freeze-drying), yielding a heated rapeseed protein extract (RP-HT) with a comparable composition as RP of 44.3% (w/w) protein and 15.2% (w/w) oil.

In another route, the protein-rich supernatant was membrane-filtrated to remove non-proteinaceous components. The result was a membrane-filtrated rapeseed protein extract (RP-MF) and a membrane-filtrated and heated rapeseed protein extract (RP-HT-MF). Here, we observe an increase in protein and oil content to 58.2–63.4% (w/w) and 21.3–21.6% (w/w) (Table 1), respectively. We want to highlight that the oleosomes possess membrane proteins that can contribute to the overall protein content, but as the protein content in oleosomes is about 3% (Romero-Guzmán, Köllmann, et al., 2020), the oleosomes will only contribute a 0.4–0.6% to the protein content, thus being negligible. Membrane filtration removed most non-proteinaceous components; an example is the phenol content, which was 6.1–7.1% (w/w) before filtration and decreased to 1.6–2.8% (w/w) afterwards. The remaining phenols in the membrane-filtrated extracts could be phenols that are bound to the proteins, but we also should keep in mind that the reagent used to quantify phenols may also bind to proteins, which might result in a slight overestimation of the phenol content. Also, membrane-filtration of RP and RP-HT reduced the ash content from 8.6-9.8% to 5.2–6.3% (w/w) and the (soluble) carbohydrate content from 24.5-24.7% to 7.2–12.3% (w/w).

The heat treatment shows a minor decrease in protein content from 63.4 to 58.2 for membrane-filtered extracts (Table 1). This is, of course, not expected, but it could be due to the attachment of denatured proteins to the surface of the tubes during the heat treatment, or due to increased membrane fouling by the proteins (Steinhauer, Marx, Bogendörfer, &

Kulozik, 2015). In addition, the heat treatment also seems to lead to a lower phenol content (1% lower for all heated treated extracts). There is a possibility that phenols interact with exposed hydrophobic sites on proteins that are formed during the heating of the proteins (Chen et al., 2021). If the heated proteins aggregate, phenols might be enclosed in the protein aggregates. The reagent might not be able to reach these enclosed phenols, thereby yielding a lower phenol content. Another possibility here is that there is less surface area of proteins (due to heat-induced aggregation) available where the reagent can bind, leading to lower values.

3.1.2. Protein solubility

The protein solubility at pH 7.0 was analysed and shown in Table 1. The protein solubility decreased from 44 to 45 to 15–17% w/w after heating. This lower solubility can most likely be attributed to heat-denatured aggregation of the proteins, which gave large aggregates that were removed in the centrifugation step when determining solubility (Barbin et al., 2011). The relatively low solubility of the RP and RP-MF is expected as the proteins were extracted at pH 9.0. At pH 7.0, the proteins are closer to their pI than at their extraction pH, leading to partial aggregation of the proteins. Ntone et al. also showed a decrease from 81% (w/w) protein solubility at pH 9.0 to about 54% (w/w) at pH 7.0 for a rapeseed protein extract similarly extracted as the RP presented here in our work (Ntone et al., 2020). This would explain the lower solubility at pH 7.0 in this work.

3.1.3. Protein denaturation properties

The heat treatment can alter the protein structure, which may be reflected in the protein denaturation properties, studied using differential scanning calorimetry (DSC) (Table 2). Peak denaturation temperatures (T_{peak}) were 94.0 and 96.0 °C, and the denaturation enthalpy was 10.2 and 9.9 J/g protein for the RP and RP-MF, respectively. The heat-treated RP-HT and RP-HT-MF only had a minor peak with a T_{peak} of 103.8 and 105.8 °C and an enthalpy of 1.4 and 0.8, respectively. The heating step of 4 s at 115 °C led to a very major reduction of the enthalphy, suggesting nearly complete denaturation of the proteins as. We also observe a shift of the T_{peak} from 94.0 to 96.0 to 103.8–105.8 °C. Our previous work showed a denaturation temperature of 90.0 for cruciferin and 107.3 for napin (Yang et al., 2020). Therefore, the T_{peak} at 94.0–96.0 °C is most likely to correspond to the cruciferin, while the peak of 103.8–105.8 °C represents the napin. This would suggest that cruciferin is mainly denatured during the heating process, and this hypothesis will be further analysed using the protein composition in section 3.2.

3.1.4. Protein surface hydrophobicity

The heating will also alter the surface hydrophobicity of the proteins, and this surface property may impact the air-water interface and foaming properties (Delahaije, Gruppen, Giuseppin, & Wierenga, 2015). The relative (rel.) surface hydrophobicity at pH 7.0 is shown in Table 2.

Table 1

The proximate composition (protein, lipid and phenol content w/w, based on dry matter), and protein solubility (% based on dry matter) at pH 7.0 of rapeseed protein extracts.

	Protein content (%)	Lipid content (%)	Phenol content (%)	Ash content (%)	Carbohydrate content (%)	Protein solubility at pH 7.0
RP	45.1 ± 0.6[a]	14.5 ± 1.1[a]	7.1 ± 0.3[d]	8.6 ± 0.2[c]	24.7 ± 2.2[c]	44.8 ± 0.9[d]
RP-HT	44.3 ± 1.0[a]	15.2 ± 1.3[a]	6.1 ± 0.3[c]	9.8 ± 0.3[d]	24.5 ± 2.9[c]	15.3 ± 0.1[a]
RP-MF	63.4 ± 0.7[c]	21.3 ± 0.6[b]	2.8 ± 0.1[b]	5.2 ± 0.7[a]	7.2 ± 2.1[a]	43.6 ± 0.1[c]
RP-HT-MF	58.2 ± 0.5[b]	21.6 ± 1.6[b]	1.6 ± 0.1[a]	6.3 ± 0.1[b]	12.3 ± 2.3[b]	17.0 ± 0.2[b]

Note.

RP: rapeseed protein extract.

RP-MF: membrane filtrated rapeseed protein extract.

RP-HR: heated rapeseed protein extract.

RP-HT-MF: heated and membrane-filtrated rapeseed protein extract.

The values shown are averages of triplicate measurements, and the standard deviations. The averages within a row with the same superscript letter are not significantly different (p > 0.05).

Table 2

Protein denaturation onset and peak temperature, denaturation enthalpy and protein surface hydrophobicity at pH 7.0 of rapeseed protein extracts.

Sample	T_{onset} (°C)	T_{peak} (°C)	Enthalpy (J/g protein)	Protein surface hydrophobicity
RP	84.9 ± 0.1[a]	94.0 ± 0.1[a]	10.2 ± 0.2[c]	0.69 ± 0.02[a]
RP-MF	86.3 ± 0.1[b]	96.0 ± 0.2[b]	9.9 ± 0.5[c]	0.74 ± 0.01[b]
RP-HT	96.2 ± 1.8[d]	103.8 ± 0.9[c]	1.4 ± 0.3[b]	0.89 ± 0.02[c]
RP-HT-MF	91.7 ± 0.2[c]	105.8 ± 0.5[d]	0.8 ± 0.1[a]	1.00 ± 0.03[d]

Note.

RP: rapeseed protein extract.

RP-MF: membrane filtrated rapeseed protein extract.

RP-HR: heated rapeseed protein extract.

RP-HT-MF: heated and membrane filtrated rapeseed protein extract.

The values shown are averages of triplicate measurements, and the standard deviations. The averages within a row with the same superscript letter are not significantly different (p > 0.05).

The values are averages of triplicate measurements, and the standard deviation is also shown. The averages within a row with the same superscript letter are not significantly different (p > 0.05).

The RP and RP-MF had a comparable relative surface hydrophobicity of 0.69 and 0.74, respectively. Heating leads to substantially higher hydrophobicity, which is expected as previously non-surface available hydrophobic sites are likely to be exposed upon heating (Y. Wang et al., 2020). Interestingly, the membrane-filtrated extracts seem to have a slightly higher hydrophobicity. A possible explanation is the occupation of the hydrophobic sites on the proteins by non-proteinaceous material in the non-membrane-filtrated extracts. These are most likely the main rapeseed protein, sinapic acid, which could bind to proteins by non-covalently via hydrophobic interactions of the phenol's phenyl-ring with hydrophobic domains on the protein surface (Cao, Xiong, Cao, & True, 2018; Jiang, Zhang, Zhao, & Liu, 2018; Kieserling et al., 2024). Consequently, the hydrophobic probing molecules will not be able to bind on the sites which are occupied by phenols, thus giving a lower hydrophobicity for non-membrane filtrated RP and RP-HT. After removal of these phenols by membrane filtration, the sites will be available for the hydrophobic probes to bind, leading to higher surface hydrophobicity.

3.2. Protein profile and size

The protein composition was analysed using sodium dodecyl sulfate – polyacrylamide gel electrophoresis (SDS-PAGE). The full extract (with soluble and insoluble protein) was first analysed for all four rapeseed protein extracts. Here, the reducing conditions are shown, for the SDS-PAGE gel obtained using non-reducing conditions, we refer to Fig. S1 in the supplementary material, where we observed similar findings as gels obtained under reducing conditions. For all extracts, we observe similar profiles with two distinct areas: 1) between 22 and 33 kDa, which are the building blocks of a cruciferin monomer, the α- and β-subunits and 2) between 4 and 8 kDa, which are the building blocks of napin, the light and heavy chain (Wanasundara, 2011). Cruciferin is expected to exist as a hexamer of around 300 kDa at a pH of 7.0, while napin is a monomer of 15 kDa (Wanasundara, 2011). At reducing conditions, these structures fall apart into the earlier-mentioned subunits and chains. Napin and cruciferin are present in the extracts, which is expected, as we omit the iso-electric point precipitation in the mild protein extraction method. A final observation is the band shown in the wells of the heated protein extracts (RP-HT and RP-MF-HT), which are largely aggregated proteins that were not broken up under reducing conditions, thus not being able to enter the pores of the gel.

While the composition of the full extract is similar for all extracts, we

see more considerable differences when only analysing the soluble fraction (at pH 7.0), where the insoluble fraction was removed using centrifugation. The insoluble fraction was visible on the first four lanes, as the reducing agent DTT breaks the dissulphide bonds between the aggregated proteins into smaller subunits. The soluble fraction of RP and RP-MF are similar, with the abundant presence of both cruciferin and napin. Heating changes the lanes of the soluble fraction of RP-HT and RP-MF-HT, as the cruciferin bands nearly disappeared, while the napin bands are still largely unaffected. These findings demonstrate that cruciferin is mainly affected in the heat treatment, as this protein is denatured and aggregated. The lower heat stability of cruciferin is expected, as it has a lower denaturation temperature (90.0 °C) than napin (107.3 °C). With the 4 s heat treatment at 115 °C, we expect a nearly complete denaturation of cruciferin, as 115 °C is far above the denaturation temperature. Napin might be only partially denatured based on the DSC results in section 3.1.3, giving dominant napin bands in the SDS-PAGE scan. In short, the result is a heat-treated rapeseed protein extract (RP-HT and RP-MF-HT) with insoluble cruciferin and (partly) soluble napin.

The formation of heat-denatured insoluble cruciferin aggregates upon denaturation is confirmed by the results of laser diffraction measurements, as presented in Fig. 3. The particle size distribution of the full extracts is shown in Fig. 3. RP and RP-MF show distributions with a large particle size population <1 μm, and one >1 μm. RP-MF shows an additional peak around 100 μm, which suggest more aggregation compared to RP. This might be related to a concentration effect, as shown for bovine serum albumin proteins, which started to aggregate at high shear and (rapid) supersaturation (thus concentration), induced during membrane filtration (Kim, Chen, & Fane, 1993). The >1 μm peak is expected to be insoluble protein aggregates, which are expected to be present, as we have shown a large portion of insoluble proteins (Table 1). In addition, oleosomes (natural oil droplets from rapeseed) can be present with sizes varying from 2 to 300 μm (Romero-Guzmán, Petris, et al., 2020). The smaller size population (0.02–1 μm) is expected to be native rapeseed proteins and smaller protein aggregates. This peak vastly decreases when the heat treatment is performed to produce RP-HT and RP-HT-MF, which confirms the heat-induced denaturation and the subsequent protein aggregation, as the >1 μm peaks grow substantially.

3.3. Interfacial properties

3.3.1. Adsorption behaviour and interfacial thickness

The adsorption behaviour of the rapeseed protein extracts was analysed for 1 h using drop tensiometry. The surface pressure over time is shown in Fig. 4A. In all further analysis, we decided to focus on standardised soluble protein fractions to allow a fair comparison between the rapeseed protein extracts. In the production of the soluble fraction, oleosomes are removed in the syringe filtration step (see section 2.2.3.) (Yang, Berton-Carabin et al., 2021). Therefore, the impact of lipids is not included in this study. The impact of oleosomes on rapeseed protein air-water interface and foaming properties was evaluated in previous studies (Yang, Berton-Carabin et al., 2021; Yang et al., 2020).

All protein extracts show an immediate surface pressure increase, as the surface pressures at 1s of adsorption varied from 5.3 to 10.5 mN/m, demonstrating the rapid adsorption of rapeseed proteins into the air-water interface. The unheated RP and RP-MF had a similar surface pressure of 5.3 and 5.7 mN/m at 1 s, and the heated RP-HT and RP-HT-MF showed a coinciding trend with surface pressures of 10.3 and 10.5 mN/m at 1 s. The surface pressure was higher for heated rapeseed protein extracts in the first 50 s, which could be related to the more hydrophobic surface of the proteins after the heat treatment. In addition, the protein composition could also play a role, as the heated extracts are rich in napin, while the unheated ones have both napin and cruciferin proteins. In previous work, Shen et al. demonstrated more rapid adsorption of napin than cruciferin in the sub-second regime (Shen,

Yang, Nikiforidis, Mocking-Bode, & Sagis, 2023). The rapid adsorption of napin could have been accelerated even more due to the heat treatment in the current work.

The main presence of napin on the air-water interface can be confirmed using ellipsometry by determining the thickness of the air-water interfacial film (insert in Fig. 4A) (Poirier, Stocco, Kapel, In, & Ramos, 2021). The interfacial thickness of the non-heated RP and RP-MF was 6.6 and 6.9 nm, respectively, which is about double the thickness of the heated RP-HT and RP-HT-MF with a value of 3.2 nm for both interfaces. In our previous work, we determined the air-water interfacial thickness of air-water interfaces stabilised by pure cruciferin and napin, which was 6.9 nm for cruciferin and 2.7 nm for napin (Shen et al., 2023). These values remarkably coincide with the thicknesses found for our interfaces, suggesting that the non-heated RP- and RP-MF-stabilised interface have formed a layer dominated by cruciferin. Of course, we should keep in mind that the measured thickness is an average over the area of the laser spot (several μm^2). Cruciferin seems to largely dominate the thickness for the non-heated interfaces, but the presence of napin cannot be excluded. Napin is presumably the dominant protein for the heated RP-HT and RP-HT-MF. We do observe a slightly higher thickness of 3.2 nm for the heated extracts compared to 2.7 nm for pure napin. Some soluble cruciferin might still be present in the heated extract, as the SDS-PAGE shows light bands for cruciferin (Fig. 2). Another possibility is the slight aggregation of napin, resulting in a slightly thicker interfacial film.

Another clear difference is the development of the surface pressure over time (Fig. 4A), especially when comparing the non-membrane and membrane-filtrated extracts. The RP has a surface pressure of 21.3 mN/m after 1 h of adsorption, while the membrane-filtered RP-MF has a value of 19.2 mN/m. For the heated extracts, a similar trend is shown as the surface pressure after 1 h of adsorption decreases from 19.9 to 16.4

Fig. 2. SDS-PAGE profile under reducing conditions containing a marker with corresponding molecular weights in kDa. The rapeseed protein extract (RP), membrane filtrated rapeseed protein extract (RP-MF), heated rapeseed protein extract (RP-HT) and heated and membrane filtrated rapeseed protein extract (RP-HT-MF) was analysed by including the full extract (soluble and insoluble protein) and by separately measuring the soluble protein.

mN/m. The non-proteinaceous solutes, typically removed via membrane filtration, seem to increase the surface pressure of the whole mixture. The main phenol in rapeseed is sinapic acid, which was previously shown to be surface active and could co-adsorb with proteins at the air-water interface (Yang, Lamochi Roozalipour, et al., 2021). Another possibility is a higher salt content in the non-membrane filtered extracts, giving solutions with higher ionic strength. A slight increase in ionic strength can reduce the protein's surface charge and increase the adsorption rate onto the interface (Qiao, Miller, Schneck, & Sun, 2021).

In summary, heating of the rapeseed protein extracts leads to an increase of surface pressure in the initial adsorption phase (<50 s), where napin seems to be the dominant protein at the air-water interface, while the non-heated samples have cruciferin-dominated interfaces. Removing non-proteinaceous solutes by membrane filtrated leads to slightly lower surface activity.

3.3.2. Surface dilatational deformations

The mechanical properties of the air-water interfacial films were analysed using dilatational surface rheology. Here, an amplitude sweep is performed, where the deformation amplitude of the air-water interface is increased stepwise from 5 to 30%. The elastic (E_d') and viscous (E_d'') components of the surface dilatational moduli are shown in Fig. 4B. The presence of both the E_d' and E_d'' suggests a viscoelastic behaviour, and the higher E_d' compared to E_d'' indicates a predominantly solid-like behaviour (Sagis & Fischer, 2014). Therefore, all rapeseed protein extracts form air-water interfacial films with a viscoelastic solid-like behaviour. The RP-stabilised interface had the lowest moduli of all extracts, which decreased from 19.8 mN/m at 5% deformation to 18.2 mN/m at 30% deformation. Removing the non-proteinaceous solutes leads to higher E_d' values for RP-MF, with values between 24.2 (5%) and 23.0 (30%) mN/m. The highest E_d' values were found for the heated samples, as the E_d' values were between 26.3 (5%) and 21.6 (30%) mN/m and between 30.0 (5%) and 21.2 (30%) mN/m for RP-HT and RP-HT-MF, respectively. Also here, membrane filtration led to higher E_d' values. Higher E_d' values indicate a stiffer air-water interface. This observation would suggest that the non-proteinaceous components reduce the interfacial stiffness, as removal by membrane filtration gives higher E_d'. Heating also led to a substantial increase in surface dilatational moduli.

We will discuss these findings in the next section, as we will introduce another analysis method by plotting Lissajous (or Lissajous-Bowditch) plots (Ewoldt, Winter, Maxey, & McKinley, 2010). All graphs show a decrease in E_d' when increasing the deformation amplitude. This deformation-dependent behaviour of the moduli suggests microstructure changes, such as disruption of the microstructure, at larger deformations. The large deformations are clearly in the non-linear viscoelastic regime. These non-linearities are neglected in the calculation of the surface moduli. Lissajous plots can be used to analyse these non-linearities, giving additional insights into the formed interfacial films. For an extensive overview of the theory of Lissajous plots, we refer to previous works (de Groot, Yang, & Sagis, 2023; Sagis, Humblet-Hua, & van Kempen, 2014).

3.3.3. Lissajous plots

Lissajous plots for 5 and 30% deformation of all protein extracts are shown in Fig. 5. The plots move in a clockwise, with the upper and lower parts of the plot representing the extension and compression cycle, respectively. The shape of the plots reflects the nature of the interface: a linear purely elastic response appears as a straight line, while a fully viscous response forms a circle. A viscoelastic interface results in an ellipsoidal plot, asshown at 5% deformation (Fig. 5A–D). The slope of the these plots indicates the interfacial stiffness, with a higher slope indicating a stiffer interface. The E_d'-values are useful to quantify these slopes. The width of the ellipse is a measure of the intra-cycle viscous dissipation.

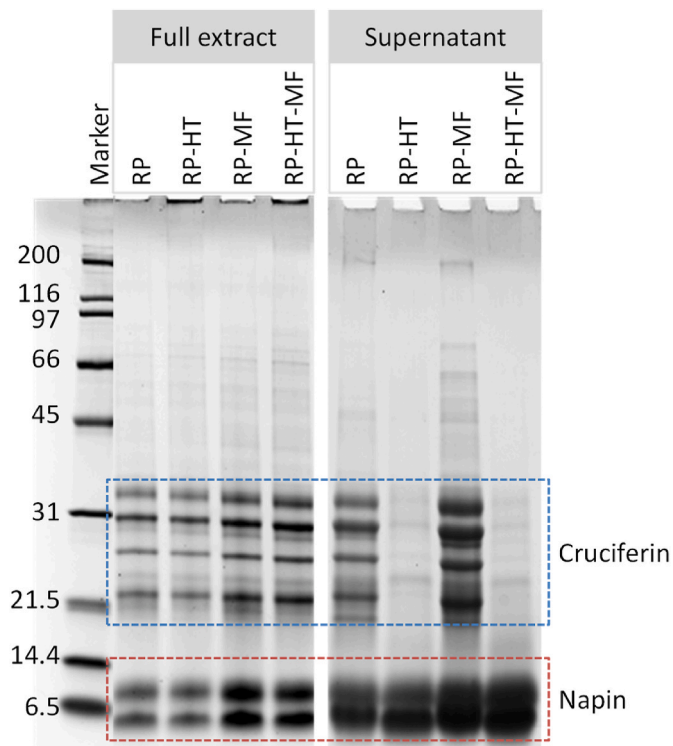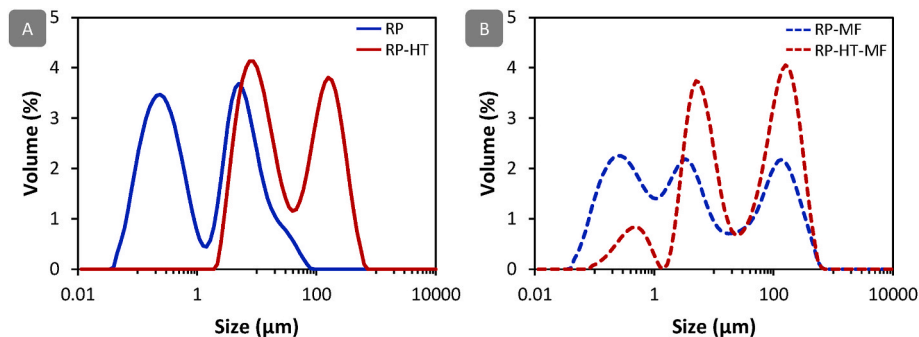At 5% deformation, the RP-stabilised interface (Fig. 5A) has the

Fig. 3. The particle size distribution of solutions prepared with rapeseed protein extract (RP), membrane-filtrated rapeseed protein extract (RP-MF), heated rapeseed protein extract (RP-HT) and heated and membrane-filtrated rapeseed protein extract (RP-HT-MF) at pH 7.0. The average of three replicate measurements (that overlap) is shown.
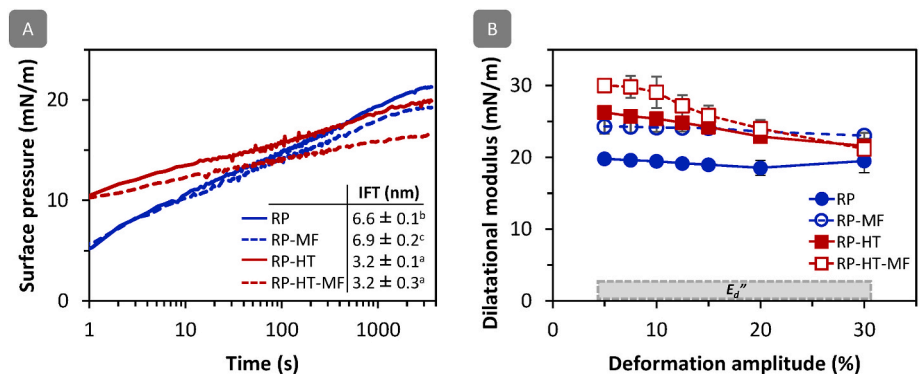

Fig. 4. (A) The surface pressure over time of 0.1% (soluble protein w/w) rapeseed protein extract (RP), membrane filtrated rapeseed protein extract (RP-MF), heated rapeseed protein extract (RP-HT) and heated and membrane filtrated rapeseed protein extract (RP-HT-MF) at an air-water interface at pH 7.0. An insert is added with the interfacial thickness (IFT) (B) The surface dilatational moduli over deformation amplitude of air-water interfacial films stabilised by the aforementioned rapeseed protein extracts. The surface elastic (E_d') and viscous (E_d'') are shown in panel B. For panel A, one representative surface pressure curve is shown, but comparable graphs were obtained in triplicate measurements. The IFT values are averages of triplicate measurements, and the standard deviation is also shown. The averages within a row with the same superscript letter are not significantly different ($p > 0.05$). For panel B, the average and error bars of moduli are obtained from at least triplicate measurement.
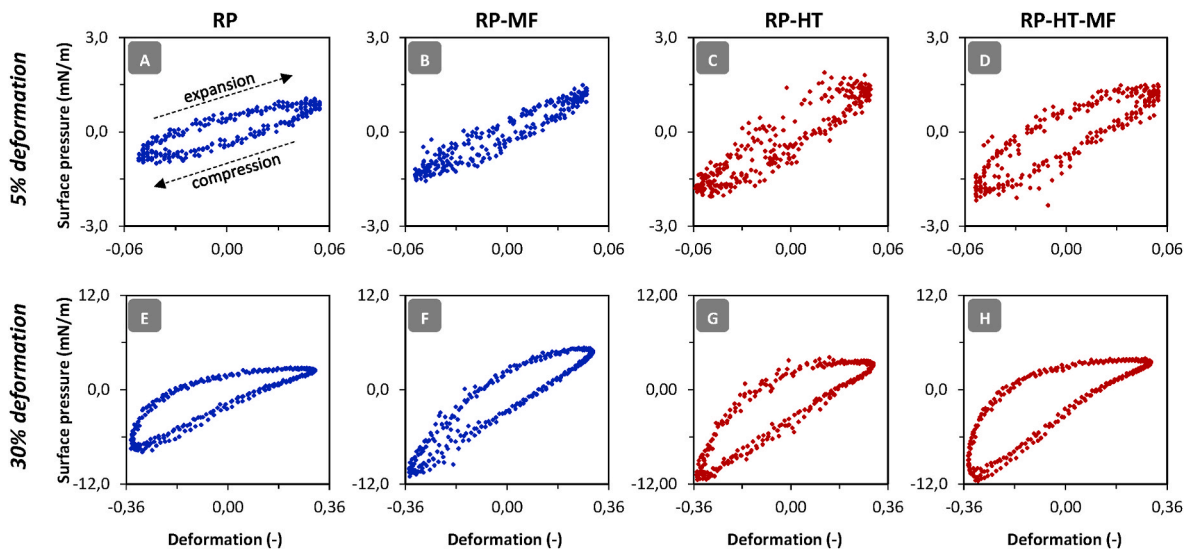

Fig. 5. Lissajous plots of surface pressure over deformation of 0.1% (soluble protein w/w) rapeseed protein extract (RP), membrane filtrated rapeseed protein extract (RP-MF), heated rapeseed protein extract (RP-HT) and heated and membrane filtrated rapeseed protein extract (RP-HT-MF)-stabilised air-water interfacial films at pH 7.0 after 1 h of aging. The shown plot is a representative plot from tripliate measurements.

smallest slope, again confirming the weakest interface formed by RP. The other extracts (Fig. 5B–D) have a higher slope, indicating stiffer interfaces; and also start showing a more non-ellipsoidal and asymmetric shape, indicating a more non-linear response. These non-linearities are more obviously present at a larger deformation of 30% (Fig. 5E–F).

At 30% deformation, the Lissajous plot of an RP-stabilised interface (Fig. 5E) shows a strong asymmetry, which is reflected as a distinct behaviour in the extension and compression of the interface. We observe a steep increase of the surface pressure at the start of the extension cycle (deformation of −0.33) and this is followed by a gradual decrease in the slope, with a near horizontal curve at the end of the extension cycle (deformation of +0.30). This indicates a strain-softening response of the interfacial microstructure during extension. In the compression cycle, the 30% plot of the RP-stabilised interface (Fig. 5E) shows a steep decrease in surface pressure from 2 mN/m to −8 mN/m, which is known as strain hardening in compression. When looking at the interfacial microstructure, we would expect an increase in the interfacial protein concentration upon interfacial compression, leading to dense aggregated protein clusters, which can start jamming. The opposite impact on protein density is expected during extension, where the proteins are diluted at the surface. The observed phenomena in extension and compression were shown for pure rapeseed protein napin and cruciferin (Shen et al., 2023). This work performed frequency sweeps, showing weak power-law behaviour, which is typical for soft disordered solid materials. The combination of these results may suggest the formation of a viscoelastic solid-like layer by proteins in RP.

Heating RP results in substantially increased strain hardening in compression (30% plot, Fig. 5G), suggesting the formation of even denser protein clusters at the end of the compression cycle, thus a stiffer interface. These denser clusters can result from stronger in-plane attractive forces between the adsorbed proteins that we may attribute to the higher protein surface hydrophobicity of the proteins after heating (Table 2). After heating, we expect more napin in the soluble fraction, as most of the cruciferin forms insoluble aggregates. In previous work, napin formed slightly weaker surfaces than cruciferin and a cruciferin-napin mixture (Shen et al., 2023). This is not the case in our work, thereby implying the possible presence of cruciferin, but also the impact of heating, which could enhance the hydrophobic forces between adsorbed napin, giving stiffer interfaces.

Membrane filtration, thus removing non-proteinaceous solutes, gives a a sizable change in the 30% deformation plots when comparing RP (Fig. 5E) to RP-MF (Fig. 5F) and RP-HT (Fig. 5G) to RP-MF-HT (Fig. 5H). The RP-MF-stabilised air-water interface (Fig. 5F) had a more extensive strain hardening in compression than the RP-stabilised one (Fig. 5E). Suggesting stronger in-plane interactions between adsorbed proteins, as explained in the previous paragraph. On the other hand, the RP-MF-HT (Fig. 5H) showed a much steeper surface pressure increase at the start of the extension cycle compared to RP-HT (Fig. 5G). This behaviour is likely the result of stronger in-plane interactions, as a steeper increase would result from a more compressed surface. In both cases, the non-proteinaceous components seem to reduce the interactions between proteins at the interface, probably hindering the proteins from approaching each other. We expect phenols to play the central role here in the disturbance of the protein interface. For instance, rapeseed phenol sinapic acid vastly reduced the interfacial stiffness of whey proteins (Yang, Lamochi Roozalipour et al., 2021). Other phenols, such as green tea phenols, showed the same impact on protein-stabilised interfaces (Rodríguez, von Staszewski, & Pilosof, 2015; von Staszewski, Pizones Ruiz-Henestrosa, & Pilosof, 2014). Additionally, phenols could bind to proteins before adsorption, thereby weakening protein-stabilised interfaces. The soluble carbohydrates (mostly small sugars) are not expected to play a prominent role here—neither are the lipids, as we remove the lipids with the syringe filtration step.

In summary, all extracts can form viscoelastic solid-like interfacial layers, where in-plane interactions between adsorbed proteins are expected. The least purified and processed RP formed the weakest air-water interface due to the presence of non-proteinaceous solutes. The negative impact of these components is also shown for the heated samples, as removal of it gives much stiffer interfaces. Finally, heating leads to the formation of the stiffest interfaces, probably due to stronger hydrophobic interactions. The processes impact the composition and protein molecular properties, again affecting the interfacial properties.

3.4. Foaming properties

The foaming ability and stability of the rapeseed protein extracts were studied by analysing the overrun and foam volume half-life time, respectively (Raymundo, Empis, & Sousa, 1998). The overrun is a measure of foaming ability, expressing the amount of foam created from a specific volume. The overrun (Fig. 6A) was comparable for all extracts (having all the same amount of soluble protein) with values between 335 and 365 %. In the foam formation phase, a new interfacial area is created that needs to be stabilised by surface active components (mainly proteins). In Fig. 4A, we show a high surface pressure already after 1 s of adsorption time. This adsorption onto the air-water interface in the sub-second regime is crucial in stabilising the newly created interface. Of course, the interface also needs to remain stable enough to avoid the collapse of the interface and foam during whipping, which requires interaction between the surface active components, as shown in the rheology section of this work (section 3.3.2.). The rapeseed protein extracts quickly adsorb at the air-water interface, giving high overrun values, comparable to whey and egg proteins (Yang, Kornet, et al., 2022). We do observe a minor but significant increase in foam overrun for the heated protein fractions, likely due to the higher protein surface hydrophobicity, and, therefore, faster adsorption behaviour for RP-HT
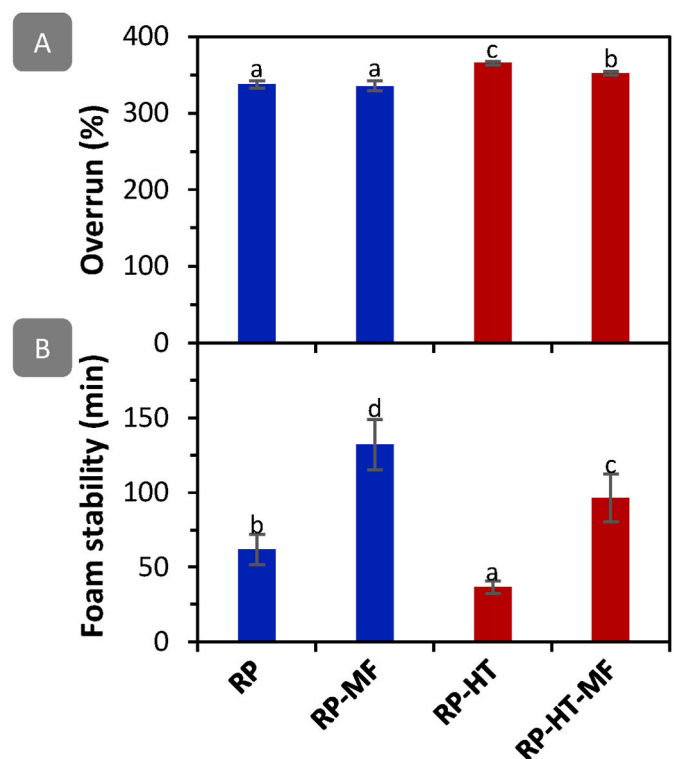

Fig. 6. (A) Foam overrun and (B) foam volume half-life time of 0.1% (soluble protein w/w) of a rapeseed protein extract (RP), membrane filtrated rapeseed protein extract (RP-MF), heated rapeseed protein extract (RP-HT) and heated and membrane filtrated rapeseed protein extract (RP-HT-MF) at pH 7.0. The values are averages of triplicate measurements, and the standard deviation is shown as error bars. The averages within a panel with the same superscript letter are not significantly different (p > 0.05).

and RP-HT-MF (Fig. 4A).

The stiffness of the air-water interface also influences the foam stability (Fig. 6B), where we observe a larger variation than in the overrun. The RP and RP-HT showed the shortest half-life times of 62 and 37 min, respectively, while membrane-filtration, thus the removal of non-proteinaceous components, nearly triples the stability to 132 min and 96 min, for RP-MF and RP-MF-HT, respectively. Membrane filtration removes the non-proteinaceous components (which reduce the in-plane interactions of proteins) so that the interfacial stiffness of the MF proteins is larger (Fig. 4B). A stronger viscoelastic interface around the air bubble could potentially slow down the bubble rupture, leading to higher foam stability.

The heated samples showed a 30–40% decrease in foam half-life time compared to the non-heated samples. This lower foam stability after heating could be related to the presence of napin at the air-water interface, as cruciferin is insoluble upon heat-induced aggregation. In previous work, cruciferin and napin were isolated, and the authors showed lower foam stability of napin (23 min) compared to cruciferin (220 min) (Shen et al., 2023). They showed a tenfold lower foam stability of a napin-dominated foam, which was not observed in our work, when comparing heated to non-heated systems in our work. This could result from the heating step, which could have led to stronger hydrophobic forces between proteins at the interface, thus giving a stiffer interfacial film and higher foam stability, compared to a native napin system. The dominance of albumins after heating an albumin-globulin mixture was previously also shown for pea and quinoa (Van de Vondel, Janssen, Wouters, & Delcour, 2023; Yang, Mocking-Bode, et al., 2022).

In summary, the membrane filtration step seems to be crucial in removing non-proteinaceous components that impair interface and foam stabilisation. The direct steam injection (DSI) aggregates cruciferin, and also increases hydrophobicity to napin. The latter is able to form stable foams. The heavy aggregation of cruciferin may be a drawback of the DSI method. The effect of these aggregates is now not incorporated in this study, as we only focused on the soluble fraction of the heated samples, mainly containing napin. A combination with other methodologies may lead to reduced aggregation, thus increased functionality. An example is enzymatic hydrolysis of rapeseed proteins, such as hydrolysis into smaller proteins, which improved foamability and stability at basic, neutral and acidic pHs after minor hydrolysis (Larré et al., 2006). Another type of hydrolysis with potential in functionality improvement is enzymatic acylation of rapeseed proteins (Sánchez-Vioque, Bagger, Larré, & Guéguen, 2004). On the other hand, the aggregation of proteins can also be used as a tool to increase foaming properties (Amagliani, Silva, Saffon, & Dombrowski, 2021). But here aggregate concentration, sizes and shapes are needed, as demonstrated for dairy protein aggregate stabilised foams, where aggregate amounts of >90% and of >117 nm reduced foam stability (Rullier, Novales, & Axelos, 2008). This suggests that by carefully tuning the heating step (DSI), the foaming properties of aggregates can be controlled.

4. Conclusions

We studied the relationship between processing history (direct stream injection and membrane filtration) and air-water interface/foam-stabilising properties of rapeseed protein extracts containing cruciferin and napin proteins, and potentially lipids and phenols. The cruciferin protein fraction formed insoluble aggregates upon heating, while the napin fraction remained soluble. This impacted the air-water interfacial film, where the native cruciferin-dominated the interface. When the cruciferin was aggregated, the napin dominated the interface. No major differences was found for the foaming propreties for heated and non-heated rapeseed protein extracts.

Membrane filtration showed a more significant impact on the functionality of the rapeseed protein extracts, as the process removes non-proteinaceous solutes (e.g. carbohydrates, phenols, and minerals),

thereby substantially increasing protein purity. Non-proteaceous components hinder the protein interfacial film formation, weakening interfacial films. Removing these impurities by membrane filtration increased the interfacial stiffness immensely, thus nearly tripling the foam stability.

The removal of small non-proteinaceous solutes plays a major role in increasing the foaming properties, which can also reduce the off-flavours and potential colour changes caused by phenols in the extracts. Membrane filtration of an unheated rapeseed protein extract gives the best-performing protein extract in foams. Heating has the main drawback of heat-induced aggregation of cruciferin, which induces lower protein solubility. But, heating is necessary to reduce enzymatic activity and ensure the microbial safety of the protein ingredient. An additional feature of heating could be the removal of undesired volatiles (off-flavours) using direct steam injection. Careful heating is required to avoid extensive protein aggregation and lower protein solubility. While aggregated proteins might not be desired for foaming applications, some applications (e.g. meat analogues or thickening) might require aggregated proteins, which should receive attention in future work. Finally, one should keep in mind that this study merely focused on the soluble protein fraction, thus removing insoluble aggregates and lipids, which should receive more attention as a complex mixture in future works. The findings in our work show the importance of understanding how protein processing history (of processes such as direct steam injection and membrane filtration) affects protein functionality, which showcases how protein ingredients can be produced with specific functional properties to create sustainable foods. To bridge these findings to application, it is determine the economical and environmental impact of such processing compared to traditional methods, which should receive attention in future works.

CRediT authorship contribution statement

Panayiotis Voudouris: Writing – original draft, Methodology, Investigation, Formal analysis. **Helene C.M. Mocking-Bode:** Validation, Methodology, Investigation. **Leonard M.C. Sagis:** Writing – review & editing. **Constantinos V. Nikiforidis:** Writing – review & editing, Supervision. **Marcel B.J. Meinders:** Writing – review & editing, Methodology, Conceptualization. **Jack Yang:** Writing – original draft, Visualization, Validation, Methodology, Investigation, Formal analysis, Conceptualization.

Declaration of competing interest

The authors have declared that no competing interest exist. This manuscript has not been published and is not under consideration for publication in any other journal. All authors approve this manuscript and its submission to Food Hydrocolloids.

Acknowledgements

Appendix A. Supplementary data

Supplementary data to this article can be found online at https://doi.org/10.1016/j.foodhyd.2024.110754.

Data availability

Data will be made available on request.

References

Aider, M., & Barbana, C. (2011). Canola proteins: Composition, extraction, functional properties, bioactivity, applications as a food ingredient and allergenicity - a practical and critical review. *Trends in Food Science and Technology, 22*(1), 21–39. https://doi.org/10.1016/j.tifs.2010.11.002

Aiking, H., & de Boer, J. (2018). The next protein transition. *Trends in Food Science and Technology, 105*(July 2018), 515–522. https://doi.org/10.1016/j.tifs.2018.07.008

Alashi, A. M., Blanchard, C. L., Mailer, R. J., & Agboola, S. O. (2013). Technological and bioactive functionalities of canola meal proteins and hydrolysates. *Food Reviews International, 29*(3), 231–260. https://doi.org/10.1080/87559129.2013.790046

Amagliani, L., Silva, J. V. C., Saffon, M., & Dombrowski, J. (2021). On the foaming properties of plant proteins: Current status and future opportunities. *Trends in Food Science & Technology, 118*(PA), 261–272. https://doi.org/10.1016/j.tifs.2021.10.001

Baker, P. W., Višnjevec, A. M., Krienke, D., Preskett, D., Schwarzkopf, M., & Charlton, A. (2022). Pilot scale extraction of protein from cold and hot-pressed rapeseed cake: Preliminary studies on the effect of upstream mechanical processing. *Food and Bioproducts Processing, 133*, 132–139. https://doi.org/10.1016/j.fbp.2022.03.007

Barbin, D. F., Natsch, A., & Müller, K. (2011). Improvement of functional properties of rapeseed protein concentrates produced via alcoholic processes by thermal and mechanical treatments. *Journal of Food Processing and Preservation, 35*(3), 369–375. https://doi.org/10.1111/j.1745-4549.2009.00476.x

Cao, Y., Xiong, Y. L., Cao, Y., & True, A. D. (2018). Interfacial properties of whey protein foams as influenced by preheating and phenolic binding at neutral pH. *Food Hydrocolloids, 82*, 379–387. https://doi.org/10.1016/j.foodhyd.2018.04.020

Chen, D., Zhu, X., Ilavsky, J., Whitmer, T., Hatzakis, E., Jones, O. G., et al. (2021). Polyphenols weaken pea protein gel by formation of large aggregates with diminished noncovalent interactions. *Biomacromolecules, 22*(2), 1001–1014. https://doi.org/10.1021/acs.biomac.0c01753

Chéreau, D., Videcoq, P., Ruffieux, C., Pichon, L., Motte, J. C., Belaid, S., et al. (2016). Combination of existing and alternative technologies to promote oilseeds and pulses proteins in food applications. *OCL - Oilseeds and Fats, Crops and Lipids, 41*(1). https://doi.org/10.1051/ocl/2016020

Cheung, L., Wanasundara, J., & Nickerson, M. T. (2014a). Effect of pH and NaCl on the emulsifying properties of a napin protein isolate. *Food Biophysics, 10*(1), 30–38. https://doi.org/10.1007/s11483-014-9350-7

Cheung, L., Wanasundara, J., & Nickerson, M. T. (2014b). The effect of pH and NaCl levels on the physicochemical and emulsifying properties of a cruciferin protein isolate. *Food Biophysics, 9*(2), 105–113. https://doi.org/10.1007/s11483-013-9323-2

de Groot, A., Yang, J., & Sagis, L. M. C. (2023). Surface stress decomposition in large amplitude oscillatory interfacial dilatation of complex interfaces. *Journal of Colloid and Interface Science, 638*, 569–581. https://doi.org/10.1016/j.jcis.2023.02.007

Delahaije, R. J. B. M., Gruppen, H., Giuseppin, M. L. F., & Wierenga, P. A. (2015). Towards predicting the stability of protein-stabilized emulsions. *Advances in Colloid and Interface Science, 219*, 1–9. https://doi.org/10.1016/j.cis.2015.01.008

Ewoldt, R. H., Winter, P., Maxey, J., & McKinley, G. H. (2010). Large amplitude oscillatory shear of pseudoplastic and elastoviscoplastic materials. *Rheologica Acta, 49*(2), 191–212. https://doi.org/10.1007/s00397-009-0403-7

Eze, C. R., Kwofie, E. M., Adewale, P., Lam, E., & Ngadi, M. (2022). Advances in legume protein extraction technologies: A review. *Innovative Food Science and Emerging Technologies, 82*(September), Article 103199. https://doi.org/10.1016/j.ifset.2022.103199

Fetzer, A., Herfellner, T., & Eisner, P. (2019). Rapeseed protein concentrates for non-food applications prepared from pre-pressed and cold-pressed press cake via acidic precipitation and ultrafiltration. *Industrial Crops and Products, 132*, 396–406. https://doi.org/10.1016/j.indcrop.2019.02.039

Geerts, M., Nikiforidis, C. V., van der Goot, A. J., & van der Padt, A. (2017). Protein nativity explains emulsifying properties of aqueous extracted protein components from yellow pea. *Food Structure, 14*, 104–111. https://doi.org/10.1016/j.foostr.2017.09.001

Gonzalez-Perez, S., Vereijken, J. M., van Koningsveld, G. A., Gruppen, H., & Voragen, A. G. J. (2005). Physicochemical Properties of 2S albumins and the corresponding protein isolate from Sunflower (Helianthus annuus). *Food Chemistry and Toxicology, 70*(1), C98–C103.

Jia, W., Curubeto, N., Rodríguez-Alonso, E., Keppler, J. K., & van der Goot, A. J. (2021). Rapeseed protein concentrate as a potential ingredient for meat analogues. *Innovative Food Science and Emerging Technologies, 72*(May), Article 102758. https://doi.org/10.1016/j.ifset.2021.102758

Jiang, J., Zhang, Z., Zhao, J., & Liu, Y. (2018). The effect of non-covalent interaction of chlorogenic acid with whey protein and casein on physicochemical and radical-scavenging activity of in vitro protein digests. *Food Chemistry, 268*(May), 334–341. https://doi.org/10.1016/j.foodchem.2018.06.015

Kieserling, H., Sagu, S. T., Schwarz, K., Keppler, J., Yang, J., Güterbock, D., et al. (2024). Protein – phenolic interactions and reactions : Discrepancies , challenges , and opportunities. *Comprehensive Reviews in Food Science and Food Safety, 23*, 1–28. https://doi.org/10.1111/1541-4337.70015

Kim, K. J., Chen, V., & Fane, a G. (1993). Aggregation during ultrafiltration. *Biotechnology, 42*, 260–265.

Kornet, R., Shek, C., Venema, P., Jan van der Goot, A., Meinders, M., & van der Linden, E. (2021). Substitution of whey protein by pea protein is facilitated by specific fractionation routes. *Food Hydrocolloids, 117*, Article 106691. https://doi.org/10.1016/j.foodhyd.2021.106691

Kornet, R., Veenemans, J., Venema, P., van der Goot, A. J., Meinders, M., Sagis, L., et al. (2021). Less is more: Limited fractionation yields stronger gels for pea proteins. *Food Hydrocolloids, 112*, Article 106285. https://doi.org/10.1016/j.foodhyd.2020.106285

Larré, C., Mulder, W., Sánchez-Vioque, R., Lazko, J., Bérot, S., Guéguen, J., et al. (2006). Characterisation and foaming properties of hydrolysates derived from rapeseed isolate. *Colloids and Surfaces B: Biointerfaces, 49*(1), 40–48. https://doi.org/10.1016/j.colsurfb.2006.02.009

Mariotti, F., Tomé, D., & Mirand, P. P. (2008). Converting nitrogen into protein - beyond 6.25 and Jones' factors. *Critical Reviews in Food Science and Nutrition, 48*(2), 177–184. https://doi.org/10.1080/10408390701279749

Nehmeh, M., Rodriguez-Donis, I., Cavaco-Soares, A., Evon, P., Gerbaud, V., & Thiebaud-Roux, S. (2022). Bio-Refinery of oilseeds: Oil extraction, secondary metabolites separation towards protein meal valorisation—a review. *Processes, 10*(5). https://doi.org/10.3390/pr10050841

Ntone, E., Bitter, J. H., & Nikiforidis, C. V. (2020). Not sequentially but simultaneously: Facile extraction of proteins and oleosomes from oilseeds. *Food Hydrocolloids, 102*, Article 105598. https://doi.org/10.1016/j.foodhyd.2019.105598

Ntone, E., Kornet, R., Venema, P., Meinders, M. B. J., van der Linden, E., Bitter, J. H., et al. (2022). Napins and cruciferins in rapeseed protein extracts have complementary roles in structuring emulsion-filled gels. *Food Hydrocolloids, 125* (August 2021), Article 107400. https://doi.org/10.1016/j.foodhyd.2021.107400

Ntone, E., Qu, Q., Gani, K. P., Meinders, M. B. J., Sagis, L. M. C., Bitter, J. H., et al. (2022). Sinapic acid impacts the emulsifying properties of rapeseed proteins at acidic pH. *Food Hydrocolloids, 125*(October 2021), Article 107423. https://doi.org/10.1016/j.foodhyd.2021.107423

Osborne, T. B. (1924). *The vegetable proteins.* Longmans green and co.

Ozdal, T., Capanoglu, E., & Altay, F. (2013). A review on protein-phenolic interactions and associated changes. *Food Research International, 51*(2), 954–970. https://doi.org/10.1016/j.foodres.2013.02.009

Pelgrom, P. J. M., Boom, R. M., & Schutyser, M. A. I. (2014). Functional analysis of mildly refined fractions from yellow pea. *Food Hydrocolloids, 44*, 12–22. https://doi.org/10.1016/j.foodhyd.2014.09.001

Peng, D., Yang, J., Groot, A. De, Jin, W., Deng, Q., Li, B., et al. (2024). Soft gliadin nanoparticles at air/water interfaces : The transition from a particle-laden layer to a thick protein film. *Journal of Colloid and Interface Science, 669*(December 2023), 236–247. https://doi.org/10.1016/j.jcis.2024.04.196

Pietrysiak, E., Smith, D. M., Smith, B. M., & Ganjyal, G. M. (2018). Enhanced functionality of pea-rice protein isolate blends through direct steam injection processing. *Food Chemistry, 243*(September 2017), 338–344. https://doi.org/10.1016/j.foodchem.2017.09.132

Poirier, A., Stocco, A., Kapel, R., In, M., & Ramos, L. (2021). Sunflower proteins at air − water and oil − water interfaces. *Langmuir, 37*, 2714–2727. https://doi.org/10.1021/acs.langmuir.0c03441

Qiao, X., Miller, R., Schneck, E., & Sun, K. (2021). Influence of salt addition on the surface and foaming properties of silk fibroin. *Colloids and Surfaces A: Physicochemical and Engineering Aspects, 609*, Article 125621. https://doi.org/10.1016/j.colsurfa.2020.125621. September 2020.

Raymundo, A., Empis, J., & Sousa, I. (1998). Method to evaluate foaming performance. *Journal of Food Engineering, 36*(4), 445–452. https://doi.org/10.1016/S0260-8774(98)00063-6

Reig, M., Vecino, X., & Cortina, J. L. (2021). Use of membrane technologies in dairy industry: An overview. *Foods, 10*(11), 1–29. https://doi.org/10.3390/foods10112768

Rodríguez, S. D., von Staszewski, M., & Pilosof, A. M. R. (2015). Green tea polyphenols-whey proteins nanoparticles: Bulk, interfacial and foaming behavior. *Food Hydrocolloids, 50*, 108–115. https://doi.org/10.1016/j.foodhyd.2015.04.015

Romero-Guzmán, M. J., Köllmann, N., Zhang, L., Boom, R. M., & Nikiforidis, C. V. (2020). Controlled oleosome extraction to produce a plant-based mayonnaise-like emulsion using solely rapeseed seeds. *Lwt, 123*, Article 109120. https://doi.org/10.1016/j.lwt.2020.109120

Romero-Guzmán, M. J., Petris, V., De Chirico, S., di Bari, V., Gray, D., Boom, R. M., et al. (2020). The effect of monovalent (Na+, K+) and divalent (Ca2+, Mg2+) cations on rapeseed oleosome (oil body) extraction and stability at pH 7. *Food Chemistry, 306* (July 2019), Article 125578. https://doi.org/10.1016/j.foodchem.2019.125578

Rommi, K., Ercili-Cura, D., Hakala, T. K., Nordlund, E., Poutanen, K., & Lantto, R. (2015). Impact of total solid content and extraction pH on enzyme-aided recovery of protein from defatted rapeseed (Brassica rapa L.) press cake and physicochemical properties of the protein fractions. *Journal of Agricultural and Food Chemistry, 63*(11), 2997–3003. https://doi.org/10.1021/acs.jafc.5b01077

Rullier, B., Novales, B., & Axelos, M. A. V. (2008). Effect of protein aggregates on foaming properties of β-lactoglobulin. *Colloids and Surfaces A: Physicochemical and Engineering Aspects, 330*(2–3), 96–102. https://doi.org/10.1016/j.colsurfa.2008.07.040

Sagis, L. M. C., & Fischer, P. (2014). Nonlinear rheology of complex fluid-fluid interfaces. *Current Opinion in Colloid & Interface Science, 19*(6), 520–529. https://doi.org/10.1016/j.cocis.2014.09.003

Sagis, L. M. C., Humblet-Hua, K. N. P., & van Kempen, S. E. H. J. (2014). Nonlinear stress deformation behavior of interfaces stabilized by food-based ingredients. *Journal of Physics: Condensed Matter, 26*(46), 9. https://doi.org/10.1088/0953-8984/26/46/464105

Sánchez-Vioque, R., Bagger, C. L., Larré, C., & Guéguen, J. (2004). Emulsifying properties of acylated rapeseed (Brassica napus L.) peptides. *Journal of Colloid and Interface Science, 271*(1), 220–226. https://doi.org/10.1016/j.jcis.2003.10.028

Sánchez-Vioque, R., Bagger, C. L., Rabiller, C., & Guéguen, J. (2001). Foaming properties of acylated rapeseed (Brassica napus L.) hydrolysates. *Journal of Colloid and Interface Science, 244*(2), 386–393. https://doi.org/10.1006/jcis.2001.7932

Sari, Y. W., Mulder, W. J., Sanders, J. P. M., & Bruins, M. E. (2015). Towards plant protein refinery: Review on protein extraction using alkali and potential enzymatic assistance. *Biotechnology Journal, 10*(8), 1138–1157. https://doi.org/10.1002/biot.201400569

Schmitt, C., Silva, J. V., Amagliani, L., Chassenieux, C., & Nicolai, T. (2019). Heat-induced and acid-induced gelation of dairy/plant protein dispersions and emulsions. *Current Opinion in Food Science, 27*, 43–48. https://doi.org/10.1016/j.cofs.2019.05.002

Shen, P., Yang, J., Nikiforidis, C. V., Mocking-Bode, H. C. M., & Sagis, L. M. C. (2023). Cruciferin versus napin – air-water interface and foam stabilizing properties of rapeseed storage proteins. *Food Hydrocolloids, 136*, Article 108300. https://doi.org/10.1016/j.foodhyd.2022.108300

Steinhauer, T., Marx, M., Bogendörfer, K., & Kulozik, U. (2015). Membrane fouling during ultra- and microfiltration of whey and whey proteins at different environmental conditions: The role of aggregated whey proteins as fouling initiators. *Journal of Membrane Science, 489*, 20–27. https://doi.org/10.1016/j.memsci.2015.04.002

Tzeng, Y., Diosady, L. L., & Rubin, L. J. (1988). Preparation of rapeseed protein isolates using ultrafiltration, precipitation and diafiltration. *Canadian Institute of Food Science and Technology Journal, 21*(4), 419–424. https://doi.org/10.1016/S0315-5463(88)70979-7

Tzeng, Y., Diosady, L. L., & Rubin, L. J. (1990). Production of canola protein materials by alkaline extraction, precipitation, and membrane processing. *Journal of Food Science, 55*(4), 1147–1151. https://doi.org/10.1111/j.1365-2621.1990.tb01619.x

Van de Vondel, J., Janssen, F., Wouters, A. G. B., & Delcour, J. A. (2023). Air-water interfacial and foaming properties of native protein in aqueous quinoa (Chenopodium quinoa Willd.) extracts: Impact of pH- and heat-induced aggregation. *Food Hydrocolloids, 144*(December 2022), Article 108945. https://doi.org/10.1016/j.foodhyd.2023.108945

Van Kempen, S. E. H. J., Schols, H. A., Van Der Linden, E., & Sagis, L. M. C. (2013). The effect of diesters and lauric acid on rheological properties of air/water interfaces stabilized by oligofructose lauric acid monoesters. *Journal of Agricultural and Food Chemistry, 61*(32), 7829–7837. https://doi.org/10.1021/jf4018355

von Staszewski, M., Pizones Ruiz-Henestrosa, V. M., & Pilosof, A. M. R. (2014). Green tea polyphenols-β-lactoglobulin nanocomplexes: Interfacial behavior, emulsification and oxidation stability of fish oil. *Food Hydrocolloids, 35*, 505–511. https://doi.org/10.1016/j.foodhyd.2013.07.008

Wanasundara, J. P. D. (2011). Proteins of brassicaceae oilseeds and their potential as a plant protein source. *Critical Reviews in Food Science and Nutrition, 51*(7), 635–677. https://doi.org/10.1080/10408391003749942

Wang, Y., Yang, F., Wu, M., Li, J., Bai, Y., Xu, W., et al. (2020). Synergistic effect of pH shifting and mild heating in improving heat induced gel properties of peanut protein isolate. *Lwt, 131*(March), Article 109812. https://doi.org/10.1016/j.lwt.2020.109812

Wang, X., & Zhao, Z. (2023a). A mini-review about direct steam heating and its application in dairy and plant protein processing. *Food Chemistry, 408*(December 2022), Article 135233. https://doi.org/10.1016/j.foodchem.2022.135233

Wang, X., & Zhao, Z. (2023b). Structural and colloidal properties of whey protein aggregates produced by indirect tubular heating and direct steam injection. *Food Structure, 35*(February 2022), Article 100301. https://doi.org/10.1016/j.foostr.2022.100301

Xia, W., Botma, T., Sagis, L. M. C., & Yang, J. (2022). Selective proteolysis of β-conglycinin as a tool to increase air-water interface and foam stabilising properties of soy proteins. *Food Hydrocolloids, 130*, Article 107726. https://doi.org/10.1016/j.foodhyd.2022.107726

Xu, F., Pan, M., Li, J., Ju, X., Wu, J., Cui, Z., et al. (2021). Preparation and characteristics of high internal phase emulsions stabilized by rapeseed protein isolate. *Lwt, 149*(May), Article 111753. https://doi.org/10.1016/j.lwt.2021.111753

Yang, J., Berton-Carabin, C. C., Nikiforidis, C. V., van der Linden, E., & Sagis, L. M. C. (2021). Competition of rapeseed proteins and oleosomes for the air-water interface and its effect on the foaming properties of protein-oleosome mixtures. *Food Hydrocolloids, 122*, Article 107078. https://doi.org/10.1016/j.foodhyd.2021.107078

Yang, J., de Wit, A., Diedericks, C. F., Venema, P., van der Linden, E., & Sagis, L. M. C. (2022). Foaming and emulsifying properties of extensively and mildly extracted Bambara groundnut proteins: A comparison of legumin, vicilin and albumin protein. *Food Hydrocolloids, 123*, Article 107190. https://doi.org/10.1016/j.foodhyd.2021.107190

Yang, J., Faber, I., Berton-Carabin, C. C., Nikiforidis, C. V., van der Linden, E., & Sagis, L. M. C. (2020). Foams and air-water interfaces stabilised by mildly purified rapeseed proteins after defatting. *Food Hydrocolloids, 112*, Article 106270. https://doi.org/10.1016/j.foodhyd.2020.106270

Yang, J., Kornet, R., Diedericks, C. F., Yang, Q., Berton-Carabin, C. C., Nikiforidis, C. V., et al. (2022). Rethinking plant protein extraction: Albumin — from side stream to an excellent foaming ingredient. *Food Structure, 31*, Article 100254. https://doi.org/10.1016/j.foostr.2022.100254

Yang, J., Kornet, R., Ntone, E., Meijers, M. G. J., van den Hoek, I. A. F., Sagis, L. M. C., et al. (2024). Plant protein aggregates induced by extraction and fractionation processes: Impact on techno-functional properties. *Food Hydrocolloids, 155*(September 2023), Article 110223. https://doi.org/10.1016/j.foodhyd.2024.110223

Yang, J., Lamochi Roozalipour, S. P., Berton-Carabin, C. C., Nikiforidis, C. V., van der Linden, E., & Sagis, L. M. C. (2021). Air-water interfacial and foaming properties of whey protein - sinapic acid mixtures. *Food Hydrocolloids, 112*, Article 106467. https://doi.org/10.1016/j.foodhyd.2020.106467

Yang, J., Mocking-Bode, H. C. M., Hoek, I. A. F. Van D., Theunissen, M., Voudouris, P., Meinders, M. B. J., et al. (2022). The impact of heating and freeze or spray drying on the interface and foam stabilising properties of pea protein extracts : Explained by aggregation and protein composition. *Food Hydrocolloids, 133*, Article 107913. https://doi.org/10.1016/j.foodhyd.2022.107913

Yang, J., Vardar, U. S., Boom, R. M., Bitter, J. H., & Nikiforidis, C. V. (2023). Extraction of oleosome and protein mixtures from sunflower seeds. *Food Hydrocolloids, 145*, Article 109078. https://doi.org/10.1016/j.foodhyd.2023.109078

Yang, J., Yang, Q., Waterink, B., Venema, P., Vries, R. De, & Sagis, L. M. C. (2023). Physical , interfacial and foaming properties of different mung bean protein fractions. *Food Hydrocolloids, 143*, Article 108885. https://doi.org/10.1016/j.foodhyd.2023.108885

Zhang, N., Xiong, Z., Xue, W., He, R., Ju, X., & Wang, Z. (2022). Insights into the effects of dynamic high-pressure microfluidization on the structural and rheological properties of rapeseed protein isolate. *Innovative Food Science and Emerging Technologies, 80*(February), Article 103091. https://doi.org/10.1016/j.ifset.2022.103091